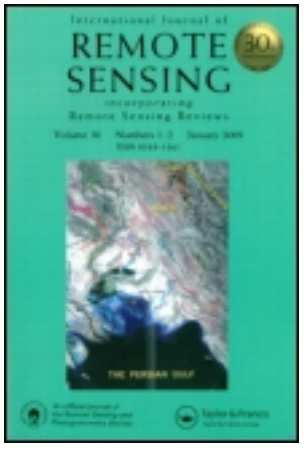

International Journal of Remote Sensing

Publication details, including instructions for authors and subscription information:
http://www.tandfonline.com/loi/tres20

Retrieval of forest chlorophyll content using canopy structure parameters derived from multi-angle data: the measurement concept of combining nadir hyperspectral and off-nadir multispectral data

Anita Simic [a], Jing M. Chen [a] & Thomas L. Noland [b]

[a] Department of Geography, University of Toronto, 100 St. George Street, Toronto, ON, M5S 3G3, Canada

[b] Ontario Ministry of Natural Resources, Ontario Forest Research Institute, 1235 Queen St. East, Sault Ste. Marie, ON, P6A 2E5, Canada

Available online: 08 Aug 2011

To cite this article: Anita Simic, Jing M. Chen & Thomas L. Noland (2011): Retrieval of forest chlorophyll content using canopy structure parameters derived from multi-angle data: the measurement concept of combining nadir hyperspectral and off-nadir multispectral data, International Journal of Remote Sensing, 32:20, 5621-5644

To link to this article: http://dx.doi.org/10.1080/01431161.2010.507257

International Journal of Remote Sensing
Vol. 32, No. 20, 20 October 2011, 5621–5644

Taylor & Francis
Taylor & Francis Group

Retrieval of forest chlorophyll content using canopy structure parameters derived from multi-angle data: the measurement concept of combining nadir hyperspectral and off-nadir multispectral data

ANITA SIMIC*†, JING M. CHEN† and THOMAS L. NOLAND‡
†Department of Geography, University of Toronto, 100 St. George Street, Toronto, ON, M5S 3G3, Canada
‡Ontario Ministry of Natural Resources, Ontario Forest Research Institute, 1235 Queen St. East, Sault Ste. Marie, ON, P6A 2E5, Canada

(*Received 23 May 2009; in final form 24 May 2010*)

The retrieval of total chlorophyll content (chl_{a+b}) per unit leaf area and unit ground area was investigated for a boreal forest near Sudbury in northern Ontario, Canada. The retrieval was based on inversions of the 5-Scale and PROSPECT models using canopy structure parameters, leaf area index (LAI) and clumping index, generated from off-nadir (multi-angle) multispectral data. Findings support the validity of combining nadir hyperspectral and multi-angle multispectral remote sensing in simultaneous retrieval of structural and biochemical vegetation parameters. Chlorophyll retrievals are improved once the improved structural parameters are obtained from multispectral data at two optimal off-nadir angles, the hotspot and darkspot. The estimated leaf chlorophyll contents agree well with the field measured values ($R^2 = 0.89$ and root mean square error (RMSE) $= 8.1\ \mu g\ cm^{-2}$). When the clumping index is excluded from the inversion, the coefficient of determination, R^2, decreases to 0.53 and the RMSE, increases to 13.4 $\mu g\ cm^{-2}$.

1. Introduction

The biochemical composition of vegetation canopies is an important indicator of ecosystem health and sustainability (Carter 1994, Lichtenthaler 1998). Leaf chlorophyll and nitrogen content are key parameters for quantifying the photosynthetic rate of foliage, and thus plant primary productivity (Ripullone *et al*. 2003, Gitelson *et al.* 2005), which influences global climate. The relationship between foliage nitrogen concentration and light-saturated photosynthesis has been widely used in physiologically based ecosystem models (Aber *et al.* 1995). Since chlorophyll content correlates to nitrogen content of forest canopies (Boggs *et al.* 2003, Gabocik 2003, Ripullone *et al.* 2003), it is used in such models to develop algorithms to estimate nitrogen content.

With remote sensing data, two approaches are commonly applied to estimate chlorophyll content: (1) the empirical–statistical approach or (2) the inversion of physically based canopy and leaf reflectance models. The former is based on correlations between hyperspectral indices, derived from reflectance at the leaf or canopy level, and chlorophyll content (Curran 1989, Elvidge and Chen 1995, Broge and Leblanc

*Corresponding author. Email: simica@geog.utoronto.ca

International Journal of Remote Sensing
ISSN 0143-1161 print/ISSN 1366-5901 online © 2011 Taylor & Francis
http://www.tandf.co.uk/journals
DOI: 10.1080/01431161.2010.507257

2001, Zarco-Tejada *et al.* 2001, le Maire *et al.* 2004, Gitelson *et al.* 2005). This approach is simple to use; however, it is site and sensor specific and does not account for the complexity of canopy structure. Although biochemical composition controls leaf and canopy reflectance properties, canopy structure (Chen *et al.* 2000) affects canopy reflectance acquired by a sensor (Gitelson *et al.* 2005, Lewis 2007, Malenovski *et al.* 2008, Verrelst *et al.* 2008). Leaves in plant canopies, especially in trees and shrubs, are generally highly clumped. Because of canopy features such as phyllotaxy, branch and shoot arrangement and crown structure, forest leaves have more vertical overlap than would occur randomly. At all sun angles, this clumping decreases the proportion of sunlit leaves and increases the proportion of shaded leaves, affecting the interaction between radiation and vegetation and thus plant growth and carbon absorption. Canopy reflectances can differ among plants that have the same canopy chlorophyll content but different canopy structure (Gitelson *et al.* 2005). This suggests that estimation of structural characteristics, clumping in particular, would help reduce uncertainties in chlorophyll content retrieval.

The latter approach, the inversion of physically based canopy and leaf models, can be used to retrieve both biophysical and biochemical vegetation parameters. These models use radiative transfer schemes that include a description of canopy architecture. Most sophisticated canopy modelling techniques, used to simulate the radiation transfer regime in a heterogeneous scene such as open forest canopies, are (1) 3-dimensional numerical models such as ray tracing (Flight, Sprint-2, Raytran and Drat), discrete ordinate (DART) and radiosity models (RGM); and (2) 3-dimensional geometric optical/hybrid models such as GORT, SGORT, LIM, 5-Scale and FRT (Pinty *et al.* 2004, Widlowski *et al.* 2007). Widlowski *et al*. (2007) reported that some 3-dimensional numerical models have matured to the point that they have been successfully validated against field measurements and provide similar results. However, these models are computationally expensive and require several input parameters. Due to their ability to capture structural vegetation parameters the geometric-optical (GO) models are more suitable for forest canopies (Chen *et al.* 2000). In such models, the canopy is represented as a collection of discrete crown entities that cast shadows onto another crown and/or the background (Gerard and North 1997, Chen *et al.* 2000). Inversion of the geometric models commonly relies on a look-up table (LUT) approach to retrieve structural components (Knyazikhin *et al.* 1998, Weiss *et al.* 2000, Combal *et al.* 2002). For instance, the GORT model was successfully inverted to estimate forest cover density (Woodcock *et al.* 1997, Ni *et al.* 1999). Zhang *et al*. (2008a) successfully inverted the 5-Scale model to calculate leaf reflectance and Lacaze and Roujean (2001) inverted the GOST model to estimate vegetation structural parameters. Coupling different types of canopy- and leaf-level models in the inversion process has been explored in studies by North (1996), Luquet *et al*. (1998), Demarez and Gastellu-Etchegorry (2000), Gastellu-Etchegorry and Bruniquel-Pinel (2001), Dawson *et al.* (2003), Kempeneers *et al.* (2008) and Verrelst *et al.* (2008).

Rapid developments in modelling approaches and remote sensing technologies over the last two decades have inspired scientists to probe the relationships between structural parameters of a vegetation canopy and multi-angle, multispectral remote sensing data. The concept of combining multi-angle and hyperspectral remote sensing, in particular, is useful to retrieve both canopy structure and biochemical parameters of vegetation (Lewis *et al.* 2001, Rautiainen *et al*. 2004, Urso *et al.* 2004, Schlerf and Hill 2005, Simic and Chen 2008, Vuolo *et al.* 2008). At fine spectral resolution, hyperspectral data provide a unique way to retrieve chlorophyll content (Curran 1989,

Elvidge and Chen 1995, Broge and Leblanc 2001, Zarco-Tejada *et al.* 2001, Gitelson *et al.* 2005). The CHRIS instrument onboard the PROBA satellite (Cutter 2004) is the first and only space-borne sensor that provides hyperspectral data at multiple viewing angles. Although improved derivation of biophysical and biochemical parameters of the surface is expected from such data, some challenges have yet to be overcome before they can be used for information retrieval. Hyperspectral measurements in single- and multiple-look directions appear to have much redundancy, and for broader application the question of which angles are best for looking at the surface remains (Costa and Fiori 2001, Bajwa *et al.* 2004, Guo *et al.* 2005, Kumar and Makkapati 2005, Vuolo *et al.* 2005).

Simic and Chen (2008) considered redundancy of multi-angle hyperspectral CHRIS data and proposed to refine the present multi-angle and hyperspectral measurement concept. They tested a new concept: a system that acquires hyperspectral signals only in the nadir direction and measures in two additional directions in two multispectral bands, red and near-infrared (NIR).

The goal of this study was to explore the applicability of this refined concept to retrieve chlorophyll content estimates from forest canopies. Simic *et al.* (2010) demonstrated that signals related to vegetation structure were strongest for a combination of two off-nadir multispectral directions, the hotspot and darkspot, and improved the retrieval of the foliage clumping index. The retrieval of chlorophyll content was derived from the Compact Airborne Spectrographic Imager (CASI) hyperspectral nadir data using the improved structural parameters, the clumping index and leaf area index (LAI), referred to as the *optimized retrieval of structural parameters*. The specific objectives of this study were:

1. To explore whether the hyperspectral signals at off-nadir angles could be successfully simulated for given nadir hyperspectral and off-nadir multispectral CASI measurements, to show that no substantial information is gained from acquiring hyperspectral measurements of vegetated areas at more than one angle.
2. To refine the inversion of 5-Scale, a geometric-optical radiative-transfer model developed by Zhang *et al.* (2008a), by incorporating the optimized retrieval of structural parameters concept of Simic *et al.* (2010).
3. To demonstrate improvements in total chlorophyll (chl_{a+b}) content retrieval per unit leaf area and unit ground area based on the hyperspectral nadir data and the optimized retrieval of structural parameters using the refined inversion model approach.

2. Modelling

The 5-Scale model is a geometric-optical radiative-transfer model that considers the structural composition of forest canopies at different scales, including tree groups, tree crown shapes, branches, shoots and leaf cells. The model can be used to simulate open canopy reflectance for all types of vegetation. A general description of what the model does is:

1. Tree crowns are simulated as discrete geometrical objects: cone and cylinder for conifers and spheroid for deciduous species. The non-random spatial distribution of trees is simulated using the Neyman type A distribution.

2. Inside the crown, branch architecture is defined by a single inclination angle (Chen and Black 1991). A branch is in turn composed of foliage elements (individual leaves in deciduous and shoots in conifer canopies) with a given angle distribution pattern.
3. The hotspot is computed both on the ground and on the foliage with gap size distributions among and within crowns, respectively.
4. The tree surface created by the crown volume (cone and cylinder or spheroid) is treated as a complex medium rather than a smooth surface so that shadowed foliage can be observed on the sunlit side and sunlit foliage on the shaded side.
5. A multiple scattering scheme that relies on view factors is used to compute the *shaded* reflectivity. This scheme is essential for hyperspectral calculations because it automatically computes a spectrum of wavelength-dependent multiple scattering factors under given canopy geometry. This makes the 5-Scale model unique for hyperspectral applications.
6. If canopy and background reflectances are available, the 5-Scale model can be used to generate the bidirectional hyperspectral reflectance at any combination of sun and view angle geometries (Leblanc *et al.* 1997, 1999).

Model parameters are separated into three groups (Leblanc *et al.* 1999) as follows: (1) site parameters–domain size equivalent to the size of a pixel, LAI, tree density, solar zenith angle (SZA), viewing angle and relative azimuth angle; (2) tree architecture parameters—crown radius and height, apex angle, needle-to-shoot ratio, foliage clumping index and typical size of tree foliage; and (3) foliage reflectance and transmittance and background reflectance spectra or band-specific reflectances and transmittance for multispectral simulations. In several studies the 5-Scale model is presented as an advanced and reliable approach for obtaining the hotspot signature (Chen *et al.* 2005, Canisius and Chen 2007, Zhang *et al*. 2008a).

To improve the performance of the 5-Scale model with respect to multi-angle simulations of background reflectance, the non-linear temporal angular model (NTAM) (Latifovic *et al.* 2003) was added to characterize the angular variation of the background reflectance measured in the field at one angle. The contributions of geometric and volume scattering are directly related to the amount of vegetation weighted through polynomial relationships for different land cover types. A complete description of the model is provided by Latifovic *et al.* (2003).

3. Methods

3.1 *Site description and field measurements*

The study area was located near Sudbury in northern Ontario (74° 09′ 47.7″ N; 81° 42′ 23.4″ W). It is a flat area at elevation of 350 m above sea level (figure 1) with three vegetation cover types: (1) mature forests of black spruce and jack pine (coniferous); (2) young jack pine trees (∼1 m high) with some open patches and shrubs (regenerating); and (3) deciduous forest patches that include mature aspen and young aspen in large canopy gaps (deciduous). During an intensive field campaign in 2007, more than 10 sites were selected in which to collect detailed ground truth data to be used in 5-Scale. However, due to the positional inconsistency between overlapping remote sensing swaths, only four of those sites were visible in all nadir and off-nadir directions.

In each of the four forest stands, measurements were performed along transects established in a 30 × 30 m plot. Effective LAI (L_e) was measured using the LAI-2000

Figure 1. Location of the study area near Sudbury, ON.

plant canopy analyser (Li-Cor, Lincoln, NE, USA). To reduce the effect of multiple scattering on the measurements the LAI-2000 was operated near dusk under diffuse radiation conditions (LAI-2000 Operating Manual 1992). The element clumping index was measured using TRAC (Tracing Radiation and Architecture of Canopies) (Chen and Cihlar 1995). Structural parameters of trees (density, height and diameter breast height) were also measured. Understorey reflectance for most common species was measured using the Field Spec Portable Spectroradiometer (ASD, Boulder, CO, USA). Measurements were made in the nadir direction around the solar noon under clear skies.

In each sample area, foliage samples were collected from the top of trees to relate the acquired reflectance by the airborne sensor to the field measured chlorophyll content. Within 10 hours of collecting the foliage, a specially designed integrating sphere, compatible with the ASD spectroradiometer, was used to measure both needle and broad leaf transmission and reflection spectra in a field laboratory. Leaves were then placed in air-tight plastic bags, refrigerated near 0°C and transported to the Ontario Forest Research Institute where leaf total chlorophyll (chl_{a+b}) content was extracted and measured using the method reported by Moorthy *et al.* (2008).

3.2 *Remote sensing data collection*

On 28 June 2007, several sets of CASI data for the study area were acquired by the Earth Observations Laboratory at York University, Toronto, ON, Canada. The CASI instrument is a push-broom airborne imager (Anger *et al.* 1994) that in this case acquired images in the hyperspectral mode in the 400–950 nm range and was flown at 105 to 129 knots at 1524 m above ground level with a 55 ms integration time. Images at the nadir view (view zenith angle (VZA) = 0°), hotspot (VZA = −40°) and darkspot (VZA = 40°) were acquired along the solar principal plane at a SZA of

about 40°. Each image had 72 bands at a spectral resolution of 7.5 nm and a spatial resolution of 3 m. York University processed the data as follows: (1) radiometric calibration of CASI images was performed using latest radiance scale factors; (2) data were atmospherically corrected to at-ground-modelled reflectance using Modtran 4 radiative transfer code in the Geomatica 10 atmospheric correction package (PCI Geomatics Richmond Hill, ON, Canada); (3) geometrical corrections were completed using geometric correction software developed by ITRES, Calgary, AB, Canada, with consideration of the roll, pitch and location information from an onboard inertia navigation system; (4) the nadir images were further corrected by locating the positions of ground control points (2 × 2 m white plastic sheets) measured in the field; and (5) the off-nadir images were further re-registered to the nadir image (from step 4) and to one another.

3.3 *Overall analytical approach*

3.3.1 Off-nadir hyperspectral reconstructions. It was explored in this study whether the hyperspectral signals at off-nadir angles could be simulated for given nadir hyperspectral and off-nadir multispectral CASI measurements. As the CASI data contain hyperspectral information acquired at multiple angles, spectral aggregation was employed to build multispectral information. The red and NIR region of the CASI data were aggregated separately within each off-nadir view based on the spectral range of the Landsat Thematic Mapper (TM) red and NIR bands, as mean reflectances of the TM bandwidths. Similarly, the mean reflectances were generated for the model-simulated spectra.

Ratios between the mean reflectances of the CASI measurements and 5-Scale model simulations for each view angle were calculated separately in red and NIR spectral regions. For each view angle, a new off-nadir hyperspectral spectrum was then reconstructed (denoted by $x_{\lambda,\text{new}}$) by multiplying the 5-Scale hyperspectral simulation with the ratios, that is, the visible region of the simulated reflectance was multiplied by the red ratio and the NIR region by the NIR ratio

$$x_{\lambda,\text{ new}} = x_{\lambda} r, \tag{1}$$

where x_{λ} is the off-nadir hyperspectral simulation value at wavelength λ and r is the ratio generated for the red or NIR spectrum. The red edge region was fine-tuned to match the corresponding red and NIR averages:

$$x_{\lambda,\text{ new}} = x_{\lambda-2} r. \tag{2}$$

These reconstructed hyperspectral values were then compared with the hyperspectral CASI measurements to show that after it is calibrated with nadir hyperspectral and off-nadir multispectral measurements, the 5-Scale model can be used to reconstruct the hyperspectral spectra at off-nadir angles.

3.3.2 Inversion of 5-Scale model and chlorophyll retrieval. The process of chlorophyll retrieval accomplished by inverting the 5-Scale and PROSPECT is illustrated in figure 2. This approach can be used to estimate leaf reflectance and chlorophyll content for varying canopy structural composition. PROSPECT (Jacquemoud and Baret 1990), the most widely used leaf radiative transfer model, simulates leaf reflectance

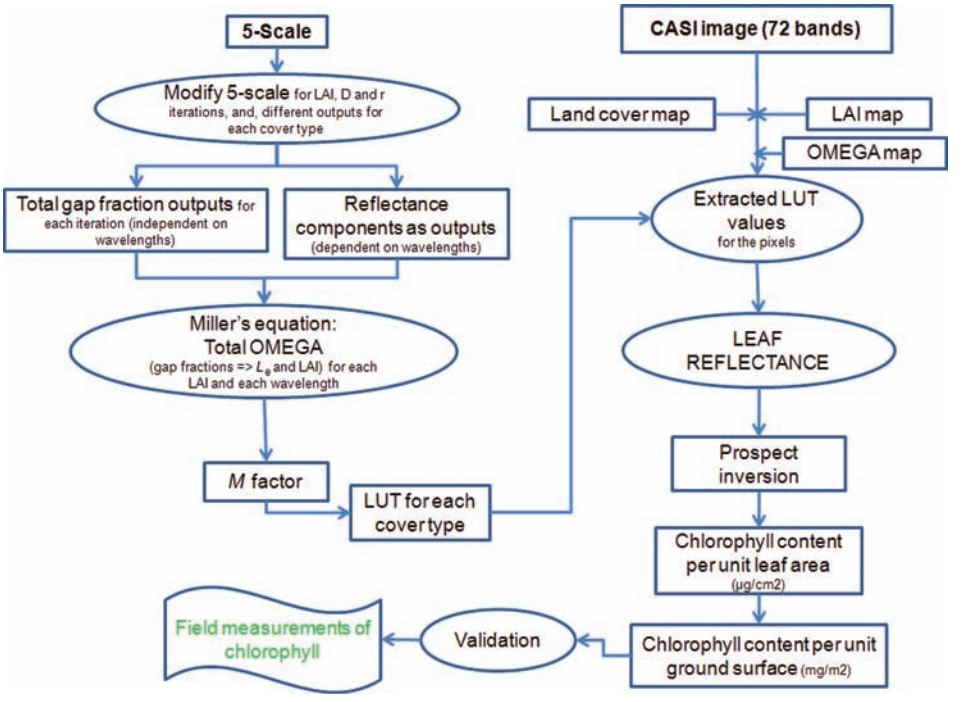

Figure 2. Steps involved in determining leaf chlorophyll content using an inverted version of the canopy reflectance model 5-Scale and the leaf reflectance model PROSPECT.

and transmittance between 400 and 2400 nm. The model assumes a leaf is a stack of N identical elementary layers separated by $N - 1$ air spaces.

First, the 5-Scale model was run in the forward mode. By combining the fine increments of the 5-Scale input structural parameters, such as LAI, tree structure and tree density, the model reflectance components were generated for each combination. These components included gap fractions, total canopy reflectance, sunlit background reflectance and the sunlit leaf and background fractions needed to calculate an M factor as explained below.

The model's forward mode does not use the total clumping index (Ω) as input but rather the element clumping index (Ω_E) as measured by TRAC (Chen 1996). For each combination of structural components the following steps were used to generate the total clumping index.

The gap fraction, $P(\theta)$, at given zenith angle θ, calculated for each combination of parameters and Miller's theorem (Miller 1967) were used to calculate the effective LAI (L_e):

$$L_e = -2 \int_0^{\pi/2} \ln[P(\theta)] \cos\theta \sin\theta \, d\theta. \tag{3}$$

The clumping index was then derived using the equation:

$$\Omega = \frac{L_e}{\text{LAI}}, \tag{4}$$

Table 1. Major parameters used to produce look-up tables (LUTs) for conifers, deciduous and regenerating forest stands.

5-Scale parameters	Mature conifers	Deciduous forest	Regenerating forest
Stick height (Ha) (m)	10	10	0.25
Crown height (Hb) (m)	2	7	1.9
Number of trees per ha (D)	500–4500	300–1750	2000–8000
Radius of crown (R) (m)	0.3–0.9	0.8–2.2	0.4–0.6
Leaf area index (LAI)	0.1–10	0.1–10	0.1–10
Solar zenith angle (SZA)	40	40	40
Element clumping index (OMEGA_E)	0.81	0.89	0.8
Needle-to-shoot ratio (GAMMA_E)	1.6	1	1.6

where LAI represents an input for a given simulation.

The average field measurements were used to parameterize the 5-Scale model (table 1).

The inversion of 5-Scale is based on the multiple scattering scheme incorporated into the model. Multiple scattering is strongest in the NIR spectral range, which may result in uncertainties in modelling canopy reflectance with geometrical optical models. As explained by Chen and Leblanc (2001), this scheme is based on view factors between sunlit and shaded components of canopy reflectance, including both foliage and background, which allows for the second and higher-order scattering simulations. Total simulated canopy reflectance (ρ) is a collection of four reflectivity components. They are combinations of sunlit foliage and background reflectances (ρ_{PT}, ρ_{PG}) and shaded foliage and background reflectances (ρ_{ZG}, ρ_{ZT}). The reflectances are weighted by the fractions/probabilities of viewing the four parts of scenes in the following manner (Chen and Leblanc 2001):

$$\rho = \rho_{PT}F_{PT} + \rho_{ZT}F_{ZT} + \rho_{PG}F_{PG} + \rho_{ZG}F_{ZG}, \tag{5}$$

where F_{PT}, F_{ZT}, F_{PG} and F_{ZG} are fractions/probabilities of viewing (from a remote sensor) sunlit tree crown, shaded tree crown, sunlit background and shaded background, respectively.

Sunlit components appear due to the first-order scattering and are enhanced by multiple scattering. On the other hand, with no multiple scattering, shaded components would be extremely dark. The multiple scattering increases both sunlit (ρ_{PT}, ρ_{PG}) and shaded (ρ_{ZG}, ρ_{ZT}) components. Therefore, the multiple scattering factor (M) is further developed in this study for the purpose of inverting reflectances from canopy to leaf.

To invert the sunlit canopy reflectance (ρ_{PT}) into the sunlit leaf reflectance (ρ_L), the sunlit canopy reflectance can be expressed as the sunlit leaf reflectance multiplied by the multiple scattering factor (M), which, in our case, includes the contributions of the two shaded components, as follows:

$$\rho_{PT} = \rho_L M. \tag{6}$$

In this case, equation (5) can be expressed as:

$$\rho = (\rho_L F_{PT})M + \rho_{PG}F_{PG}. \tag{7}$$

By re-arranging equation (7) to include the shaded components (ρ_{ZG}, ρ_{ZT}) in the M factor, the following equation is derived to calculate the M factor (Zhang *et al.* 2008a):

$$M = \frac{\rho - \rho_{PG} F_{PG}}{\rho_L F_{PT}}, \tag{8}$$

where ρ is the canopy-level total reflectance simulated by 5-Scale and ρ_L is measured leaf reflectance, which is an input value.

Other factors in equation (8) are derived using the 5-Scale model; canopy reflectance ρ can be remotely measured and forest sunlit background reflectivity (ρ_{PG}) is known. An important change from equation (5) to equation (8) is the substitution of ρ_{PT} with ρ_L. ρ_{PT} is the reflectance of sunlit crown while ρ_L is the sunlit leaf reflectance as measured in the integrating sphere in the laboratory. As the sunlit crown surface is complex at different angles to the sun, these two reflectances differ. In the 5-Scale model, the sunlit crown reflectance is calculated based on leaf reflectance, leaf–sun angle and the probability of viewing the shaded leaves on the sunlit side. To make the inversion simple and feasible, the difference between ρ_{PT} and ρ_L is absorbed into the M factor, although the difference is not due to multiple scattering. This M factor was calculated for each LAI–Ω combination and the LUTs were generated for each land cover type (conifer, deciduous and regenerating forest). For each LAI–Ω combination, the LUTs contained M factor, total canopy-level reflectance (which was replaced by CASI reflectance in the leaf reflectance estimation; see equation 9), sunlit background reflectance and the viewing fractions for sunlit foliage and background.

Given that the model-driven canopy reflectance (ρ) closely resembles remote sensing data (ρ_{CASI}) and that the M factor for a forest is provided based on equation (8), then the following equation can be used to estimate leaf reflectance of a pixel representing a forest stand

$$\rho_L = \frac{\rho_{CASI} - \rho_{PG} F_{PG}}{M_{F_{PT}}}. \tag{9}$$

The corresponding leaf reflectance values were extracted based on the LAI and Ω maps, which were generated in the optimized retrieval of structural parameters by Simic *et al.* (2010). The LAI and Ω maps represent improved structural parameters generated using the empirical approach between the clumping index and the Normalized Difference between Hotspot and Darkspot (NDHD) index (figure 3). The NDHD, an angular index, is based on the best two view angles: (i) the hotspot, where the sun and view directions coincide; and (ii) the darkspot, where the sensor sees the maximum amount of vegetation structural shadows.

The inversion of the leaf reflectance model PROSPECT (Jacquemoud and Baret 1990), modified for conifer needles (Zhang *et al.* 2008b) was used to generate leaf chlorophyll content based on the extracted leaf reflectance values. Canopy chlorophyll maps were generated by incorporating the improved LAI values (Simic *et al.* 2010).

4. Results

4.1 *Validation of simulated spectra*

As the goal was to demonstrate performance of the 5-Scale model for open and closed canopies, two of the available study sites and vegetation types (SB7b (open canopy)

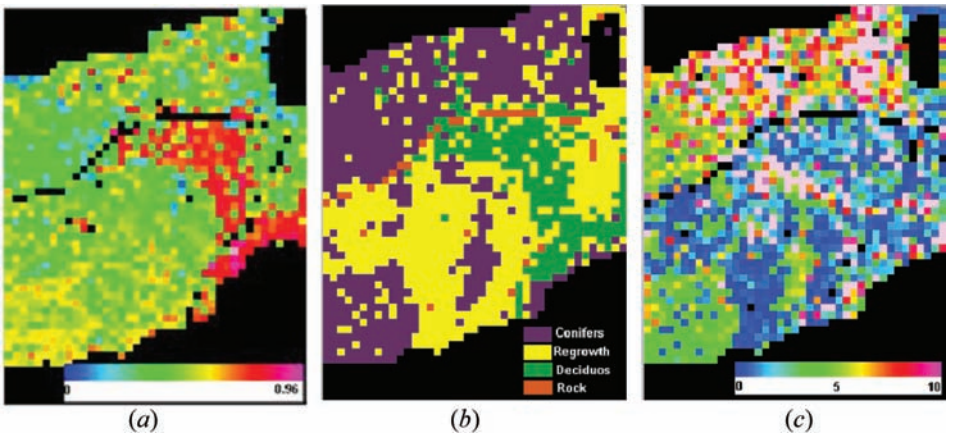

Figure 3. Maps generated by Simic *et al*. (2010) and used in this study with permission: (*a*) clumping index generated using the normalized difference between Hotspot and Darkspot (NDHD) index based on the hotspot and darkspot spectra; (*b*) land cover; (*c*) Leaf area index (LAI). Pixel size is 3 m.

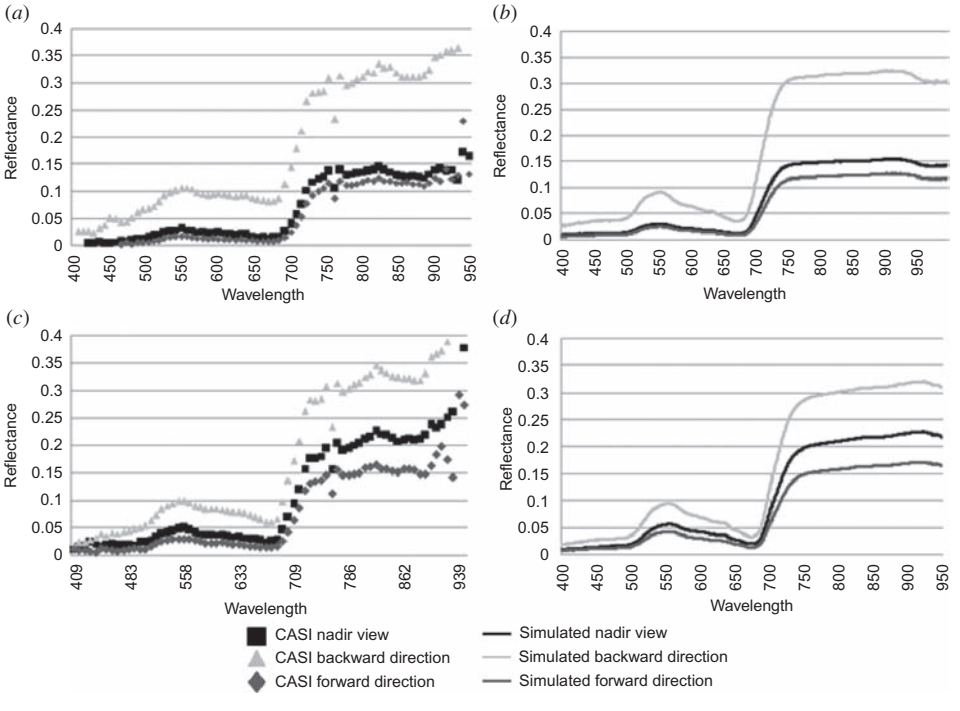

Figure 4. Agreement between the CASI spectra and 5-Scale simulations for black spruce sites SB17 ((*a*) and (*b*), respectively) and SB7b ((*c*) and (*d*), respectively) at the nadir and off-nadir directions. Backward viewing direction represents the hotspot; forward viewing direction represents the darkspot. The agreement between the off-nadir data depended on the calibration of the nadir.

and SB17 (closed canopy)) were chosen to demonstrate the agreement between CASI measurements and 5-Scale simulations (figure 4).

In all wavelengths Site SB7b had higher nadir values than site SB17 due to extensive open space, which meant more exposure of the understorey vegetation and soil

background. Pronounced forward scattering (i.e. darkspot reflectance) may result from relatively sparse vegetation and a strong influence of the background under the forest canopy (Chen and Cihlar 1996). The general trend suggests that the hotspot (i.e. backward reflectance), relative to the nadir, is smaller for a canopy with lower LAI and lower crown radius (SB7b). Even though tree density could be high, this occurs because of the increased probability of observing the ground, which has a lower reflectivity than the foliage. This trend is consistent with the finding of Chen and Leblanc (1997).

The 5-Scale model was initially calibrated against the nadir and validated against the off-nadir measurements. Although the trend of the simulated off-nadir reflectances generally coincides with the CASI measurements, some disagreement is observed between the simulated and measured hotspot reflectances within the red spectrum (figure 4). Even though the pre-processing of the CASI data was done carefully, some uncertainties, for example due to atmospheric corrections, may persist. A similar disagreement was observed for the forward reflectances of CHRIS data in the study by Simic and Chen (2008). The CASI spectra are somewhat lower than those simulated with 5-Scale by Chen and Leblanc (2001). Overall, the results show very good performance of the 5-Scale model.

4.2 *Reconstruction of off-nadir 5-Scale simulations*

As illustrated in figures 5 and 6, study results confirmed the validity of the proposed concept (section 3.3.1), and indicate that the hyperspectral information at off-nadir directions could be reconstructed from off-nadir multispectral red and NIR measurements in addition to the nadir hyperspectral data. The reconstructed hyperspectral simulation results were similar to those obtained using the CASI data for both off-nadir angles (see also table 2). Although more research is required, these agreements suggest that the hyperspectral airborne data acquired at multiple angles may include redundancy. This supports the findings reported by Simic and Chen (2008) and Simic *et al.* (2010) who proposed that the combination of the nadir hyperspectral and off-nadir multispectral data is optimal for retrieval of structural and biochemical vegetation parameters.

In addition, the measurements at off-nadir red and NIR (multispectral) reflectances are necessary to reduce or remove any biases in off-nadir hyperspectral simulations. Table 2 indicates that the mean bias errors, calculated as the absolute differences, were considerably reduced when the reconstructed simulations were compared to the CASI data. Like any other model, 5-Scale cannot perfectly represent off-nadir hyperspectral reflectance. Therefore, the calibrated nadir hyperspectral reflectance and additional off-nadir multispectral reflectance are necessary and sufficient to assure accurate model performance for both nadir and off-nadir spectral simulations.

4.3 *Model inversion*

In the inversion process, the shaded components were lumped into a single multiple scattering M factor to reduce the complexity in the inversion from canopy to leaf reflectance. The shaded components generally contributed less to the total canopy reflectance than the sunlit components and they were also less variable than the sunlit components with LAI and SZA.

Behaviour of the LUT components is summarized in table 3. The M factor decreased with the increase in LAI and with the increase in clumping index at each

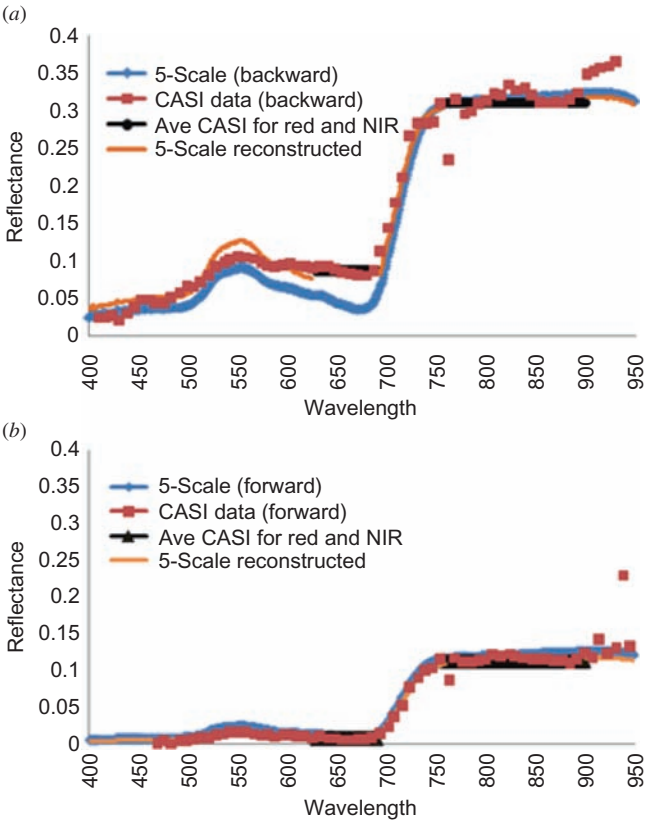

Figure 5. Reconstruction of the off-nadir spectra for black spruce (site SB17) based on CASI average reflectance in aggregated red and NIR bands for (*a*) backward viewing direction (the hotspot) and (*b*) forward viewing direction (the darkspot).

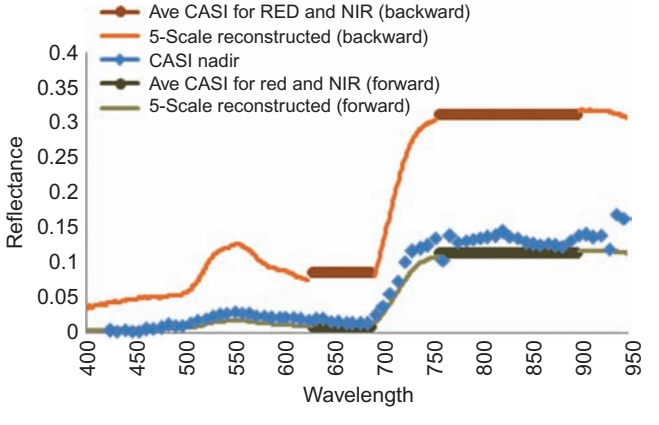

Figure 6. Reconstruction of the hotspot (backward direction) and darkspot (forward direction) based on CASI average reflectance in aggregated red and NIR bands in addition to the nadir.

Table 2. Mean bias errors (absolute difference) of the reconstructed 5-Scale simulations and the original simulations when compared to the CASI spectra.

Sensor	Site	Viewing angle (VZA)	Spectral region	Mean bias error (before reconstruction)	Mean bias error (after reconstruction)
CASI	SB17	VZA = 40	(Visible) VIS	0.0082	0.0045
			Red edge-NIR	0.0068	0.0019
		VZA = −40	(Visible) VIS	−0.0140	−0.0078
			Red edge-NIR	−0.0149	−0.0042

LAI level. This means that the contribution of the shaded components decreased as LAI increased and clumping decreased (clumping index increased). Similarly, both sunlit background reflectance and the probability of seeing sunlit background reflectance were reduced as LAI and Ω increased (table 3). In contrast, the total reflectance and the probability of seeing sunlit foliage increased with increasing LAI and Ω.

The *M* factor varied more with LAI than with the clumping index at the same LAI (figure 7). The values generally followed the shape of vegetation signature; low values (below or above 1) in the visible and high values (generally around 2 or higher) in the NIR spectral region. The magnitude and spectral variation patterns of the *M* factor resulted from multiple scattering, shaded components, and complex tree crown surfaces. The spectral variation of the *M* factor resembled leaf reflectance spectra because the second- and higher-order scattering was more or less proportional to the leaf scattering coefficient (sum of reflectance and transmittance). The magnitude was generally larger than unity to compensate for the shaded components. In the visible spectral range, the *M* factor was sometimes smaller than unity because of the conversion from ρ_{PT} to ρ_L. The complex tree crown surface (explained in section 2) allowed for shadowed foliage to be observed on the sunlit side, making ρ_{PT} smaller than ρ_L. These shadow effects sometimes overrode the effect of the *M* factor, making its value smaller than unity in the visible region (Zhang *et al.* 2008a). The variability in leaf orientation relative to sun direction also affected this trend.

Calculated leaf reflectances were similar to the input measurements. The estimated and field-measured leaf reflectances were correlated ($R^2 = 0.85$ to $R^2 = 0.98$) for given sites. Some discrepancy was observed in the blue region (400–500 nm) and beyond band 69 (916 nm) likely due to atmospheric corrections of the CASI data.

Chlorophyll content maps obtained by inverting the PROSPECT model are shown in figure 8. The chlorophyll content per unit leaf area ranged from 10 to 60 μg cm^{-2}

Table 3. Behaviour of the look-up table components.

	M factor	ρ	ρ_{PG}	F_{PT}	F_{PG}
LAI	LAI↑ = M↓	LAI↑ = ρ↑ then ρ↓	LAI↑ = ρ_{PG}↓	LAI↑ = F_{PT}↑	LAI↑ = F_{PG}↓
OMEGA	Ω↑ = M↓ within each LAI	Ω↑ = ρ↑ within each LAI	Ω↑ = ρ_{PG}↓ within each LAI	Ω↑ = F_{PT}↑	Ω↑ = F_{PG}↓

ρ is the total simulated reflectance, ρ_{PG} is sunlit background reflectance, F_{PT} and F_{PG} are fractions or probability of seeing sunlit foliage and sunlit background, respectively.

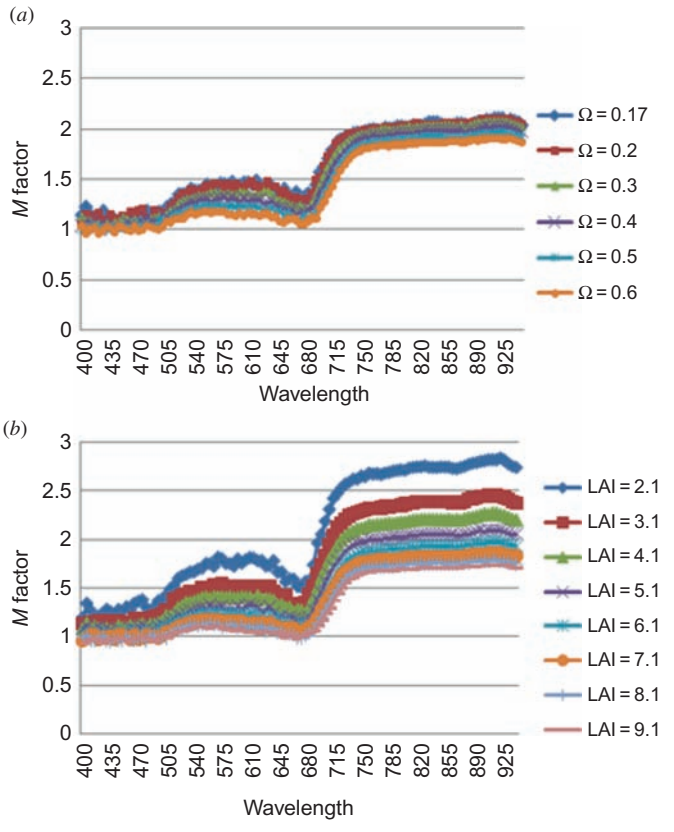

Figure 7. Variations of the *M* factor with different (*a*) clumping index (Ω) (same LAI) and (*b*) LAI (same Ω).

(figure 8(*a*)). Several pixels had higher values (> 60 μg cm^{-2}). The highest values were observed for the deciduous area (40–60 μg cm^{-2}) and some areas populated with young jack pine. The area shown in the top part of the image is populated by mature conifers and jack pine, and a mixture of high and somewhat lower chlorophyll content values (figure 8(*a*)) is evident. Overall, the results concur with the findings of other studies for forests in the Sudbury region (Moorthy *et al.* 2008, Thomas *et al.* 2008): the highest values were found for jack pine and aspen stands (generally 29–59 μg cm^{-2}) with slightly lower values for black spruce (20–45 μg cm^{-2}). The results generally agree with those reported by Zhang *et al.* (2008a). As suggested by Verrelst *et al.* (2008), a typical range of chlorophyll content for conifer leaves is 15–95 μg cm^{-2}.

The chlorophyll content per unit ground area generally ranged between 50 and 4000 mg m^{-2} (figure 8(*b*)). The lowest chlorophyll content values were obtained for the regenerating forest, which has much open area. Similarly, deciduous forest, which dominates the area on the right hand side of the image, had low chlorophyll per unit ground area, also due to their open canopies and exposed soil. The area in the top and middle portions of the image, populated with mature and healthy conifers, had high chlorophyll content per unit ground area. The values obtained in this study were somewhat higher than those reported by Zhang *et al.* (2008a). The difference is

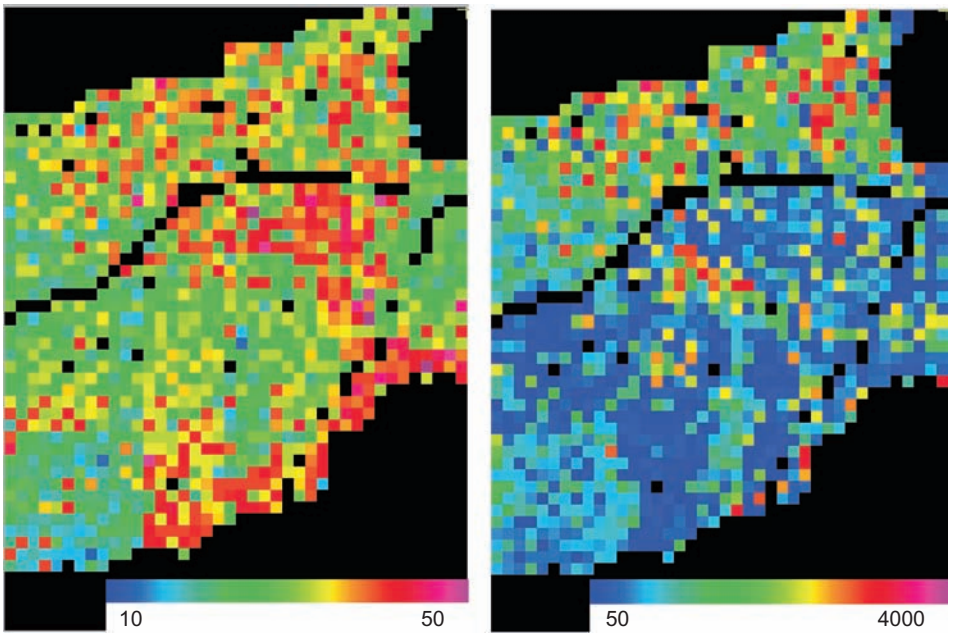

Figure 8. Chlorophyll content per (*a*) unit leaf ($\mu g\ cm^{-2}$) and (*b*) unit ground area ($mg\ m^{-2}$) based on the look-up tables, improved structural parameters and the inversion of PROSPECT. Pixel size is 3 m.

possibly due to the LAI map (figure 3). Some LAI values for conifers were slightly higher than would be expected for a small number of conifer pixels (Simic *et al.* 2010).

The coefficient of determination between the estimated and field-measured chlorophyll content per unit leaf area in our study was higher ($R^2 = 0.69$) than that reported by Zhang *et al.* (2008a) ($R^2 = 0.47$) (figure 9). And excluding the outlier in figure 9 increased the correlation coefficient to $R^2 = 0.89$. The mean values of the estimated and measured chlorophyll contents do not differ statistically at a significance level of 0.1. The proposed concept yields higher RMSE (RMSE = 8.1 $\mu g\ cm^{-2}$) than that found by Zhang *et al.* (2008a) (RMSE = 4.3 $\mu g\ cm^{-2}$). Thus, changes in observations were estimated more accurately using the proposed sampling concept than with previously documented approaches but the bias was considerable (RMSE = 8.1 $\mu g\ cm^{-2}$).

To reduce the potential bias due to chlorophyll sampling process or calibration of the remote sensing algorithms, the effect of clumping was further explored; the LUTs were generated without considering Ω.

First, they were developed LUTs based on LAI (with no other structural parameters) and estimated chlorophyll content per unit leaf area (figure 10(*a*)). Comparing these results with the field-measured data, the determination coefficient decreased to $R^2 = 0.53$ and RMSE increased to 13.4 $\mu g\ cm^{-2}$ for the per-unit-leaf case. The shift in R^2 is significant at 85% confidence interval.

Second, L_e values were employed for each site in a way that the LUT components were based on the LAI values extracted assuming $\Omega = 1$ (figure 11(*a*)). In this scenario, the coefficient of determination decreases to $R^2 = 0.29$ and RMSE increases to 22.9 $\mu g\ cm^{-2}$ in the per-unit-leaf case. The shift in R^2 from the previous case is significant at 85% confidence interval.

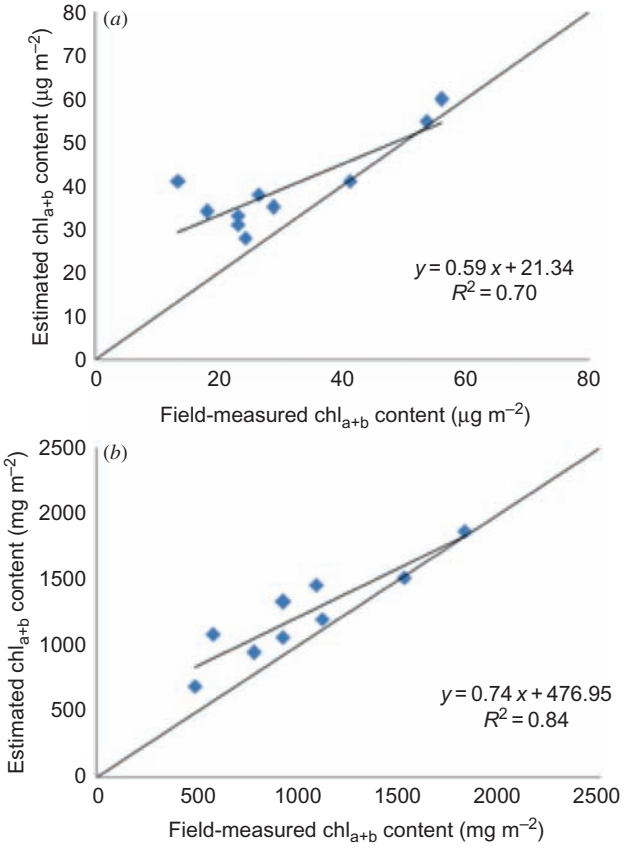

Figure 9. Correlation between field-measured and estimated chlorophyll per (*a*) unit leaf area (μg cm^{-2}) and (*b*) unit ground area (mg m^{-2}). When the outlier in (*a*) is excluded, the coefficient of determination is $R^2 = 0.89$.

Similar trends of decreased accuracy were observed for the estimated chlorophyll per unit ground area in both cases (figures 10(*b*) and 11(*b*)).

5. Uncertainties

Exposure of the understorey and soil in open forest canopies represents a major obstacle to accurately estimate leaf chlorophyll content. A background of vegetation contributes to variation in total chlorophyll and one of soil and litter can affect estimates of chlorophyll content (Verrelst *et al.* 2008). The understorey directly affects the simple ratio (SR) values, resulting in some uncertainties in the SR–LAI algorithms. Houborg and Boegh (2008) reported that even at high forest canopy density, soil reflectance affected LAI estimates due to the high canopy penetration capabilities of the NIR reflectance. Although exploring the effect of the background was not a goal of this study, it was desirable to separate the understorey and overstorey reflectances (Urso *et al.* 2004, Canisius and Chen 2007). Two steps were used in this study to reduce uncertainties related to the background. First, background reflectances, measured and averaged for each study site, were used as inputs to the model. Second, refinement of

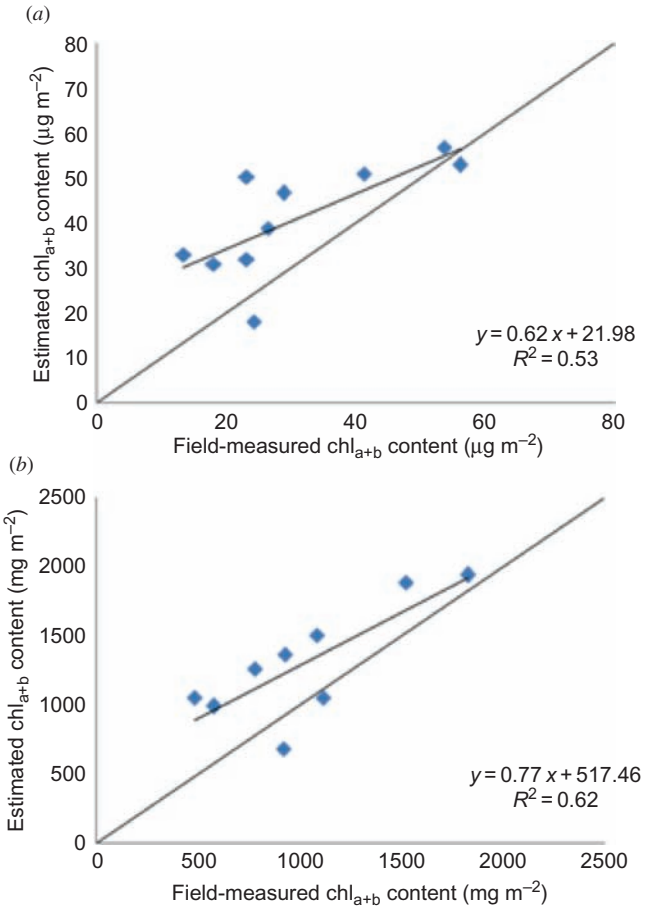

Figure 10. Correlation between field-measured and estimated chlorophyll per (*a*) unit leaf area (μg cm^{-2}) and (*b*) unit ground area (mg m^{-2}) based on LAI from the LUT when no clumping is involved.

the 5-Scale model to account for the anisotropic effect of the background, as explained in section 2, helped further to reduce the uncertainties. Although the 5-Scale model is sensitive to background reflectance, in the study by Simic *et al.* (2010) on the same sites, the structural forest components overpowered the effect of the background on the canopy reflectance measurements.

Because similar canopy spectra may be produced from different combinations of canopy structural parameters, all physically based models may be limited in their performance. This so-called *ill-posed nature* of model inversion (Combal *et al.* 2002, Atzberger 2004) can be reduced by carefully selecting the initial parameters. To a certain extent this phenomenon occurred in our study as well; different structural canopy characteristics sometimes resulted in the same total Ω values. However, by incorporating the optimized retrieval of structural parameters in the inversion process, the ill-posed nature of model inversion was minimized. Vuolo *et al.* (2008) also emphasized that multi-angular information should smooth the ill-posed problem as this technology better characterizes the anisotropy of reflectance from vegetation.

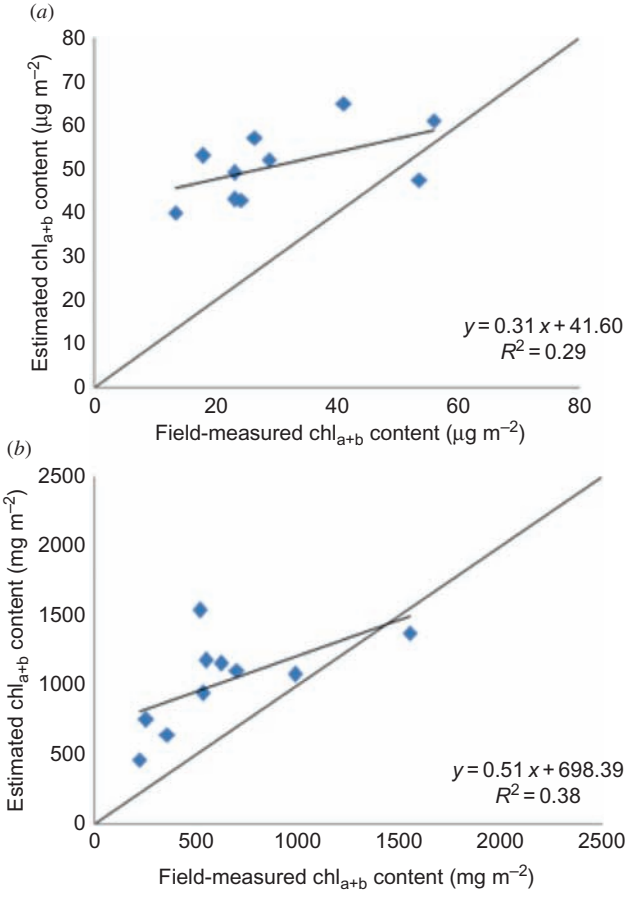

Figure 11. Correlation between field-measured and estimated chlorophyll per (*a*) unit leaf area (μg cm $^{-2}$) and (*b*) unit ground area (mg m^{-2}) based on effective LAI (L_e) (from the LUT when no clumping is involved). clumping index (Ω) is assumed to be 1.

Some CASI values in our measurements were negative in the blue region, increasing the differences between the estimated and field-measured leaf reflectance. This disagreement occurs due to the CASI reflectance behaviour, which is a result of high atmospheric scattering and related atmospheric correction in this spectral range. As chl_{a+b} was not separated into its components, the blue band spectral region is not essential to the results. Possible error issues with PROSPECT were not explored in this study. In general, higher statistical significance in results may be possible by sampling more study sites with larger ranges in LAI and chlorophyll content.

6. Discussion

The final results (figures 9–11) indicate that errors for the concept proposed in this study were considerably lower than those for the two scenarios for which the clumping index was ignored. Both random errors and accuracy were reduced by incorporating the clumping index in the model inversion. When the field-measured data were compared with the estimated values, the LAI-based relationship was more strongly

correlated than the L_e-based relationship. This suggests that the clumping index incorporated in LAI during the initial measurement steps provided better results than the L_e-based case in which the clumping index was ignored. Overall, the results demonstrated that chlorophyll content retrieval was improved when the optimized retrieval of structural parameters was considered. Demarez and Gastellu-Etchegorry (2000) found that errors in leaf chlorophyll content can exceed 23 $\mu g\ cm^{-2}$ if canopy architecture is not considered. Moorthy *et al.* (2008) showed that RMSE of the estimated chlorophyll content is reduced from 9.8 to 6.3 $\mu g\ cm^{-2}$ when shadow pixels are masked and only sunlit pixels are included in the relationships between canopy reflectance and chlorophyll content. Delegido *et al.* (2008) used a mathematical approach to relate CHRIS multi-angle reflectances and biophysical parameters in an independent retrieval of LAI and chlorophyll content. Structural and biochemical vegetation characteristics, such as clumping index and chlorophyll content, vary considerably within the same species (Houborg and Boegh 2008). Thus, the coupling of these variables is crucial for chlorophyll content retrieval in open canopy vegetation.

The chlorophyll content per unit ground area was strongly correlated ($R^2 = 0.84$) between field measured and estimated values. However, the results are still biased. The retrieval algorithms can increase the overall bias errors of the results over and above measurement and sampling errors. The spatially invariable leaf and background reflectances used as inputs to 5-Scale, and a single background reflectance data file used in the inversion may be influenced by second order errors in the multiple scattering (M factor) calculation, although they are justifiably used to avoid making the LUT construction unnecessarily complicated. This may cause deviations of the chlorophyll content estimates from the true values in a systematic manner and result in error bias. More sophisticated LUTs that compensate for variations in background greenness with effective LAI are needed to improve chlorophyll estimates.

While the random error for the laboratory method of measuring chlorophyll in our study is low (mostly less than 5%) (Noland, unpublished data), its error bias remains unknown but is expected to be small. In natural systems, tree to tree variations in chlorophyll can be quite large and choosing enough representative individual trees to get an accurate estimate of the average canopy chlorophyll per stand is critical. The reason for sampling five representative trees per stand was to get enough samples from the stand to reduce the error bias in these samples and to accurately represent the average canopy chlorophyll concentration. However, increased sampling effort should decrease the bias (Walther and Moore 2005). Differences in sampling locations and methods of choosing sample trees in this study versus that by Zhang *et al.* (2008a) may account for differences in their results.

The findings indicate the strength of the canopy model inversion approach using the M factor. Given that canopy reflectance from a sensor and background reflectance measurements are available, this innovative inversion method of calculating leaf reflectance based on the vegetation structural information appears to be reliable. This approach allows for leaf-level information retrieval in the absence of leaf spectra field measurements. The ability to estimate leaf-level information based on remote sensing data is an important step forward in hyperspectral applications to forestry including forest health, resource management and carbon cycle estimation.

7. Conclusions

This study investigated the feasibility of the recently proposed concept (Simic and Chen 2008) of combining nadir hyperspectral with hotspot and darkspot multispectral

measurements to simultaneously characterize vegetation structural and biochemical parameters from airborne CASI acquisitions. The correlation between retrieved and field-measured chlorophyll content was stronger when canopy structure parameters, such as the clumping index, were considered. The concept may be considered as a refinement of the approach used in the operation of the existing multi-angle hyperspectral sensor CHRIS. This refinement has been proposed to reduce the redundancy of hyperspectral data at more than one angle and to better retrieve the three-dimensional vegetation structural information by choosing the two most useful angles of measurement. The concept is only tested for vegetated surfaces and for visible and NIR wavelengths and further work is needed to test it for longer wavelengths and for other applications of hyperspectral data, such as soil moisture assessment and mineral exploration.

The LUT approach in the canopy reflectance model inversion developed in this study represents an elegant way to obtain sunlit leaf reflectance spectra from hyperspectral remote sensing measurements, for the purpose of leaf chlorophyll retrieval through leaf-level reflectance model inversion.

Acknowledgements

We thank the Canadian Space Agency (CSA) for funding this research. We also thank Lawrence Gray of York University for conducting airborne campaigns with the CASI instrument, and Jan Pisek and Yongqin Zhang for their help with fieldwork. In addition, Maara Packalen analysed the chlorophyll samples.

References

Aber, J.D., Ollinger, S.V., Federer, C.A., Reich, P.B., Goulden, M.L., Kicklighter, D.W., Mellilo, J.M. and Lathrop, Jr. R.G., 1995, Predicting the effects of climate change on water yield and forest production in the northeastern United States. *Clime Research*, **5**, pp. 207–222.

Anger, C.D., Mah, S. and Babey, S., 1994, Technological enhancement to the compact airborne spectrographic imager (CASI). In *Proceedings of the First International Airborne Remote Sensing Conference and Exhibition*, 10 May 1994, Strasbourg, France (Ann Arbor MI: Environmental Research Institute of Michigan), pp. 205–213.

Atzberger, C., 2004, Object-based retrieval of biophysical canopy variables using artificial neural nets and radiative transfer models. *Remote Sensing of Environment*, **93**, pp. 53–67.

Bajwa, S.G., Bajcsy, P., Groves, P. and Tian, L.F., 2004, Hyperspectral image data mining for bands selection in agricultural applications. *Transactions of the ASAE*, **47**, pp. 895–907.

Boggs, J.L., Tsegaye, T.D., Coleman, T.L., Reddy, K.C. and Fahsi, A., 2003, Relationship between hyperspectral reflectance, soil nitrate-nitrogen, cotton leaf chlorophyll, and cotton yield: a step toward precision agriculture. *Journal of Sustainable Agriculture*, **22**, pp. 5–16.

Broge, N.M. and Leblanc, E., 2001, Comparing predictive power and stability of broadband and hyperspectral vegetation indices for estimation of green leaf, area index, and canopy chlorophyll density. *Remote Sensing of Environment*, **76**, pp. 165–172.

Canisius, F. and Chen, J., 2007, Retrieving forest background reflectance in a boreal region from multi-angle imaging spectroradiometer (MISR) data. *Remote Sensing of Environment*, **107**, pp. 312–321.

Carter, G.A., 1994, Ratios of leaf reflectances in narrow wavebands as indicators of plant stress. *International Journal of Remote Sensing*, **15**, pp. 697–703.

Chen, J.M., 1996, Optically-based methods for measuring seasonal variation of leaf area index in boreal conifer stands. *Agricultural and Forest Meteorology*, **80**, pp. 135–163.

CHEN, J.M. and BLACK, T.A., 1991, Measuring leaf area index of plant canopies with branch architecture. *Agricultural and Forest Meteorology*, **57**, pp. 1–12.

CHEN, J.M. and CIHLAR, J., 1995, Plant canopy gap size analysis theory for improving optical measurements of leaf area index. *Applied Optics*, **34**, pp. 6211–6222.

CHEN, J.M. and CIHLAR, J., 1996, Retrieving leaf area index of boreal conifer forests using Landsat TM images. *Remote Sensing of Environment*, **55**, pp. 153–162.

CHEN, J.M. and LEBLANC, S.G., 1997, A four-scale bidirectional reflectance model based on canopy architecture. *IEEE Transactions on Geoscience and Remote Sensing*, **35**, pp.1316–1337.

CHEN, J.M. and LEBLANC, S.G., 2001, Multiple-scattering scheme useful for geometric optical modeling. *IEEE Transactions on Geoscience and Remote Sensing*, **39**, pp. 1061–1071.

CHEN, J.M., LI, X., NILSON, T. and STRAHLER, A., 2000, Recent advanced in geometrical optical modeling and its applications. *Remote Sensing Reviews*, **18**, pp. 227–262.

CHEN, J.M., MENGES, C.H. and LEBLANC, S.G., 2005, Global mapping of foliage clumping index using multi-angular satellite data. *Remote Sensing of Environment*, **97**, pp. 447–457.

COMBAL, B., BARET, F., WEISS, M., TRUBUIL, A., MACE, D., PRAGNERE, A., MYNENI, R., KNYAZIKHINY, Y. and WANG, L., 2002, Retrieval of canopy biophysical variables from bidirectional reflectance using prior information to solve the ill-posed inverse problem. *Remote Sensing of Environment*, **84**, pp. 1–15.

COSTA, S. and FIORI, S., 2001, Image compression using principal component neural networks. *Image and Vision Computing*, **19**, pp. 649–668.

CURRAN, P.J., 1989, Remote sensing of foliar chemistry. *Remote Sensing of Environment*, **30**, pp. 271–278.

CUTTER, M., 2004, Review of aspects associated with the CHRIS calibration. In *Proceedings of the 2nd CHRIS/PROBA Workshop*, ESA SP-578, 28–30 April 2004, Frascati, Italy (Frascati: ESRIN).

DAWSON, T.P., NORTH, P.R.J., PLUMMER, S.E. and CURRAN, P.J., 2003, Forest ecosystem chlorophyll content: implications for remotely sensed estimates of net primary productivity. *International Journal of Remote Sensing*, **24**, pp. 611–617.

DELEGIDO, J., FERNANDEZ, G., GANDIA, S. and MODENO, J., 2008, Retrieval of chlorophyll content and LAI of crops using hyperspectral techniques: application to PROBA/CHRIS data. *International Journal of Remote Sensing*, **29**, pp. 7107–7127.

DEMAREZ, V. and GASTELLU-ETCHEGORRY, J.P., 2000, A modeling approach for studying forest chlorophyll content. *Remote Sensing of Environment*, **71**, pp. 226–238.

ELVIDGE, C.D. and CHEN, Z., 1995, Comparison of broad-band and narrow-band red and near-infrared vegetation indices. *Remote Sensing of Environment*, **54**, pp. 38–48.

GABOCIK, N., 2003, Relationship between contents of chlorophyll (a+b) (SPAD values) and nitrogen of some temperate grasses. *Photosynthetica*, **41**, pp. 285–287.

GASTELLU-ETCHEGORRY, J.P. and BRUNIQUEL-PINEL, V., 2001, A modeling approach to assess robustness of spectrometric predictive equations for canopy chemistry. *Remote Sensing of Environment*, **76**, pp. 1–15.

GERARD, F.F. and NORTH, P.R.J., 1997, Analyzing the effect of structural variability and canopy-optical model. *Remote Sensing of Environment*, **62**, pp. 46–62.

GITELSON, A.A., VIÑA, A., CIGANDA, V., RUNDQUIST, D.C. and ARKEBAUER, T.J., 2005, Remote estimation of canopy chlorophyll in crops. *Geophysical Research Letters*, **32**, D08403, doi: 10.1029/2005GL0226880.

GUO, B., GUNN, S., DAMPER, B. and NELSON, J., 2005, Hyperspectral image fusion using spectrally weighted kernels. In *Proceedings of the 8th International Conference on Information Fusion*, 28 June – 1 July 2005, Philadelphia, PA (Stockholm: IEEE), pp. 402–408.

HOUBORG, R. and BOEGH, E., 2008, Mapping leaf chlorophyll and leaf area index using inverse and forward canopy reflectance modeling and SPOT reflectance data. *Remote Sensing of Environment*, **112**, pp. 186–202.

JACQUEMOUD, S. and BARET, F., 1990, PROSPECT: a model of leaf optical properties spectra. *Remote Sensing of Environment*, **34**, pp. 75–91.

KEMPENEERS, P., ZARCO-TEJADA, P.J., NORTH, P.R.J., DE BACKER, S., DELALIEUX, S., SEPULCRE-CANTO, G., MORALES, F., VAN AARDT, J.A.N., SAGARDOY, R., COPPIN, P. and SCHEUNDERS, P., 2008, Model inversion for chlorophyll estimation in open canopies from hyperspectral imagery. *International Journal of Remote Sensing*, **29**, pp. 5093–5111.

KNYAZIKHIN, Y., MARTONCHIK, J.V., MYNENI, R.B., DINER, R.J. and RUNNING, S.W., 1998, Synergistic algorithm for estimating vegetation canopy leaf area index and fraction of absorbed photosynthetically active radiation from MODIS and MISR data. *Journal of Geophysical Research*, **103**, pp. 32 257–32 276.

KUMAR, R. and MAKKAPATI, V., 2005, Encoding of multispectral and hyperspectral image data using wavelet transform and gain shape vector quantization. *Image and Vision Computing*, **23**, pp. 721–729.

LACAZE, R. and ROUJEAN, J.-L., 2001, G-function and hot spot (GHOST) reflectance model application to multi-scale airborne POLDER measurement. *Remote Sensing of Environment*, **76**, pp. 67–80.

LATIFOVIC, R., CIHLAR, J. and CHEN, J.M., 2003, A comparison of BRDF models for the normalization of satellite optical data to a standard Sun-target-sensor geometry. *IEEE Transactions on Geoscience and Remote Sensing*, **41**, pp. 1889–1898.

LEBLANC, S.G., BICHERON, P., CHEN, J.M., LEROY. M. and CIHLAR, J., 1999, Investigation of directional reflectance in boreal forests using an improved 4-Scale model and airborne POLDER data. *IEEE Transactions on Geoscience and Remote Sensing*, **37**, pp. 1396–1414.

LEBLANC, S.G., CHEN, J.M. and CIHLAR, J., 1997, Directionality of NDVI in boreal forests. *Canadian Journal for Remote Sensing*, **23**, pp. 369–380.

LE MAIRE, G., FRANCOIS, C. and DUFRENE, E., 2004, Towards universal broad leaf chlorophyll indices using PROSPECT simulated database and hyperspectral reflectance measurements. *Remote Sensing of Environment*, **89**, pp. 1–28.

LEWIS, P., 2007, 3D canopy modeling as a tool in remote-sensing research. In *Functional-Structural Plant Modeling in Crop Production*, J. Vos, L.F.M. Marcelis, P.H.B. de Visser, P.C., Struik and J.B. Evers (Eds.), pp. 219–229 (Wageningen: Springer).

LEWIS, P., BARNSLEY, M.J. and CUTTER, M., 2001, CHRIS-PROBA: mission status and prospects for mapping surface biophysical parameters. In *Proceedings of the International Geoscience and Remote Sensing Symposium (IGARSS)*, 9–13 July 2001, Piscataway, NJ (Sydney: IEEE).

LICHTENTHALER, H.K., 1998, The stress concept in plants: as introduction. *Annals of the New York Academy of Science*, **851**, pp. 187–198.

LI-COR, INC., 1992, *LAI-2000 Plant Canopy Analyzer – Operating Manual* (Lincoln, NE: LI-COR, INC.).

LUQUET, D., BEGUE, A., DUAZAT, J., NOUVELLON, Y. and REY, H., 1998, Effect of the vegetation clumping on the BRDF of semi-arid grassland: comparison of the SAIL model and ray tracing applied to a 3D computerized vegetation canopy. In *Proceedings of Geoscience and Remote Sensing Symposium (IGARSS)*, 6–10 July 1998, Piscataway, NJ (New York: IEEE), pp. 791–793.

MALENOVSKI, Z., MARTIN, E., HOMOLOVA, L., GASTELLU-ETCHEGORRY, J.P., ZURITA-MILA, R., SCHAEPMAN, M.E., POKOMY, R., CLEVERS, J.G.P.W. and CUDLIN, P., 2008, Influence of woody elements of a Norway spruce canopy on nadir reflectance simulated by the DART model at very high spatial resolution. *Remote Sensing of Environment*, **112**, pp. 1–18.

MILLER, J.B., 1967, A formula for average foliage density. *Australian Journal of Botany*, **15**, pp. 141–144.

Moorthy, I., Miller, J.R. and Noland, T.L., 2008, Estimating chlorophyll concentration in conifer needles with hyperspectral data: an assessment at the needle and canopy level. *Remote Sensing of Environment*, **112**, pp. 2824–2838.

Ni, W., Li, X., Woodcock, M., Caetano, C.E. and Stahler, A., 1999, An analytical model of bidirectional reflectance over discontinuous plant canopies. *IEEE Transactions on Geoscience and Remote Sensing*, **37**, pp. 1–13.

North, P.R.J., 1996, Three-dimensional forest light interaction model using a Monte Carlo method. *IEEE Transactions on Geoscience and Remote Sensing*, **34**, pp. 946–956.

Pinty, B., Widlowski, J.-L., Taberner, M., Gobron, N., Verstraete, M.M., Disney, M., Gascon, F., Gastellu, J.-P., Jiang, L., Kuusk, A., Lewis, P., Li. X., Ni-Meister, W., Nilson, T., North, P., Qin, W., Su, L., Tang, S., Thomson, R., Vernoef, W., Wang, H., Wang, J., Yan, G. and Zang, H., 2004, Radiation transfer model intercomparison (RAMI) exercise: results from the second phase. *Journal of Geophysical Research*, **109**, D06210, doi: 10.1029/2003JD004252.

Rautiainen, M., Stenberg, P., Nilson, T. and Kuusk, A., 2004, The effect of crown shape on the reflectance of coniferous stands. *Remote Sensing of Environment*, **89**, pp. 41–52.

Ripullone, F., Grassi, G., Lauteri, M. and Borghetti, M., 2003, Photosynthesis – nitrogen relationships: interpretation of different patterns between *Pseudotsuga menziesii* and *Populus* x *euroamericana* in mini-stand experiment. *Tree Physiology*, **23**, pp. 137–144.

Schlerf, M. and Hill, J., 2005, Estimation of forest biophysical characteristics through coupled atmosphere-reflectance model inversion using hyperspectral multi-directional remote sensing data – a contribution to future forest inventory strategies. In *Proceedings of the 3rd CHRIS/Proba Workshop*, ESA SP-593, 21–23 March 2005, Frascati, Italy (Frascati: ESRIN).

Simic, A. and Chen, J.M., 2008, Refining a hyperspectral and multiangle measurement concept for vegetation structure assessment. *Canadian Journal of Remote Sensing*, **34**, pp. 174–191.

Simic, A., Chen, J.M., Freemantle, J., Miller, J.R. and Pisek, J., 2010, Improving clumping and LAI algorithms based on multiangle airborne imagery and ground measurements. *IEEE Transactions on Geoscience and Remote Sensing*, **48**, pp. 1742–1759.

Thomas, V., Treitz, P., McCaughey, J.H., Noland, T. and Rich, L., 2008, Canopy chlorophyll concentration estimation using hyperspectral and lidar data for a boreal mixed-wood forest in northern Ontario, Canada. *International Journal of Remote Sensing*, **29**, pp. 1029–1052.

Urso, G.D., Dini, L., Vuolo, F., Alonso, L. and Guanter, L., 2004, Retrieval of leaf area index by inverting hyperspectral multi-angular CHRIS/PROBA data from SPARC 2003. In *Proceedings of the 2nd CHRIS/Proba Workshop*, ESA SP-578, 28–30 April 2004, Frascati, Italy (Frascati: ESRIN).

Verrelst, J., Schaepman, M.E. and Clevers, J.G.P.W., 2008, A modeling approach for studying forest chlorophyll content in relation to canopy composition. In *The International Archives of the Photogrammetry, Remote Sensing, and Spatial Information sciences*, **XXXVII**(Part B7), 3–11 July 2008, Beijing, China (Beijing: ISPRS Congress).

Vuolo, F., Dini, L. and Urso, G.D., 2005, Assessment of LAI retrieval accuracy by inverting a RT model and a simple empirical model with multiangular and hyperspectral CHRIS/PROBA data from SPARC. In *Proceedings of the 3rd CHRIS/Proba Workshop*, ESA SP-593, 21–23 March 2005, Frascati, Italy (Frascati: ESRIN).

Vuolo, F., Dini, L. and Urso, G.D., 2008, Retrieval of leaf area index from CHRIS/PROBA data: an analysis of the directional and spectral information content. *International Journal of Remote Sensing*, **29**, pp. 5063–5072.

Walther, B.A. and Moore, J.L., 2005, The concept of bias, precision and accuracy, and their use in testing the performance of species richness estimators, with a literature review of estimator performance. *Ecography*, **28**, pp. 815–829.

Weiss, M., Baret, F., Myneni, R.B., Pragnere, A. and Knyazikhin, Y., 2000, Investigation of a model inversion technique to estimate canopy biophysical variables from spectral and directional reflectance data. *Agronomie*, **20**, pp. 3–22.

Widlowski, J.-L., Taberner, M., Pinty, B., Bruniquel-Pinel, V., Disney, M., Fernandes, R., Gastellu–Etchegorry, J.-P., Gobron, N., Kuusk, A., Lavergne, T., Leblanc, S., Lewis, P.E., Martin, E., Mottus, M., North, P.R.J., Qin, W., Robustelli, M., Rochdi, N., Ruiloba, R., Soler, C., Thomson, R., Vernoef, W., Verstraete, M.M. and Xie, D., 2007, Third radiation transfer model intercomparison (RAMI) exercise: documenting progress in canopy reflectance models. *Journal of Geophysical Research*, **112**, D09111, doi: 10.1029/2006JD007821.

Woodcock, C.E., Collins, J.B., Jakabhazy, V.D., Li, X., McOmber, S. and Wu, Y., 1997, Inversion of the Li-Strahler canopy reflectance model for mapping forest structure. *IEEE Transactions on Geoscience and Remote Sensing*, **35**, pp. 405–414.

Zarco-Tejada, P.J., Miller, P.J., Mohammed, G.H., Noland, T.L. and Sampson, P.H., 2001, Scaling-up and model inversion methods with narrow-band optical indices for chlorophyll content estimation in closed forest canopies with hyperspectral data. *IEEE Transactions on Geoscience and Remote Sensing*, **39**, pp. 1491–1507.

Zhang, Y., Chen, J.M., Miller, J.R. and Noland, T.L., 2008a, Leaf chlorophyll content retrieval from airborne hyperspectral remote imagery. *Remote Sensing of Environment*, **112**, pp. 3234–3247.

Zhang, Y., Chen, J.M., Miller, J.R. and Noland, T.L., 2008b, Retrieving chlorophyll content in conifer needles from hyperspectral measurements. *Canadian Journal of Remote Sensing*, **34**, pp. 296–310.